

IAC-10-C2.8.1

A MEMS-BASED XYLOPHONE BAR MAGNETOMETER FOR PICO SATELLITES

S. Ranvier
Belgian Institute for Space Aeronomy, Belgium, sylvain.ranvier@aeronomie.be

V. Rochus
University of Liège, Belgium, V.Rochus@ulg.ac.be

S. Druart
Université catholique de Louvain, Belgium, sylvain.druart@uclouvain.be

H. Lamy
Belgian Institute for Space Aeronomy, Belgium, herve.lamy@aeronomie.be

P. Rochus
Centre Spatial de Liège, Belgium, prochus@ulg.ac.be

L. Francis
Université catholique de Louvain, Belgium, laurent.francis@uclouvain.be

Abstract- Initially studied and developed by students in universities, the very small pico satellites (with a mass lower than 1 Kg) are more and more considered for science applications. In particular they will be used in constellations of small spacecraft for remote sensing of various regions of the magnetosphere. They require a payload with specific size, weight and power consumption. In order to respond to this demand, new instruments have to be developed. Those instruments should exhibit at least the same performance as those used in larger satellites while fulfilling the specific requirements imposed by the size of the satellites. For this reason, we currently develop a xylophone bar magnetometer (XBM) based on micro-electromechanical systems (MEMS) with integrated detector electronics. The principle of this magnetometer is based on classical resonating xylophone bar. A sinusoidal current oscillating at the fundamental transverse resonant frequency of the bar is applied to the bar. When an external magnetic field is present, the resulting Lorentz force causes the bar to vibrate at its fundamental frequency with a displacement directly proportional to the amplitude in one direction of the ambient magnetic field. When designing a MEMS XBM, the detection method is a crucial aspect. The measurement method largely influences the geometry of the magnetometer as well as the manufacturing technology. Due to the constraints in terms of size, weight and power consumption, the two most promising measurement methods identified are capacitive and piezoelectric. Designs which include these measurement techniques are presented and simulated under realistic conditions. A new configuration of PZT/Pt structure is introduced and leads to much better sensitivity than the traditional Pt/PZT/Pt sandwich structure. The principle of the electronic circuits enabling high sensitivity and low power consumption is presented. Finally, a design including lateral electrodes for capacitive measurement is introduced.

I. INTRODUCTION

Magnetic fields play a key role in many aspects of the solar-terrestrial interactions. For example, during geomagnetic activity, charged particles precipitate along geomagnetic field lines and produce spectacular aurora. Strong sheets of fieldaligned currents (FACs) associated with these precipitations produce local perturbations of the geomagnetic field. A magnetometer onboard a spacecraft crossed by these current sheets will record the magnetic field perturbations and will provide a measure of the field aligned current using the Maxwell's equation $\vec{\nabla} \wedge \vec{B} = \vec{J}$. With a single spacecraft stationary current sheet may be obtained. However this situation is not always observed. In some cases, spatial and temporal variations of the magnetic field cannot be discriminated. Currently the separation of satellites in multi-spacecraft missions like Cluster or Themis is usually larger than the width of the current sheet. This example illustrates the importance of multipoint measurements with a fleet of micro- or pico-spacecraft with small separations.

Since launch costs represent a significant fraction of the total mission expenditures, reducing such costs necessitates careful consideration of instrument and spacecraft component miniaturization. The goal of this research is to build a sensitive, low mass, low size and low consumption magnetometer to embark onboard a fleet of micro-, nano- or pico-satellites in order to carry out these multi-point measurements. Three main types of magnetometers have been traditionally used in space missions: the fluxgate magnetometer (FGM), the search-coil magnetometer (SCM) and the vector helium magnetometer (VHM). Efforts to miniaturize size and mass of these magnetic sensors have been limited by fabrication difficulties and loss of sensitivity. Therefore, we are developing another type of magnetomer: a Xylophone Bar Magnetometer (XBM), in which the displacement of a beam is directly proportional to the magnitude of one component of the ambient magnetic field. The specific design of this magnetometer makes it particularly suitable to be fabricated using Microelectromechanical Systems (MEMS) technology. This study benefits from previous works initiated at the Applied Physics Laboratory of the John Hopkins University (Givens et al 1996, Wickenden et al 1997, Zanetti et al 1998, Oursler et al 1999, Wickenden et al 2003). The challenging task with this XBM is to reach the subnanotesla accuracy and qualify it for space applications.

Measuring the amplitude of the deflection of the bar is a crucial aspect in the development of such a device. The measurement method largely influences the geometry of the magnetometer as well as the manufacturing technology. Basically, the measurement method has to be decided before starting the design of the magnetometer. Due to size, weight and power consumption constraints, the two most promising measurement methods identified are piezoelectric and capacitive. Designs which include these measurement techniques are analyzed in Section III and IV, respectively.

All the simulations presented in this paper were performed using the finite element method (FEM) and were carried out with the software *Oofelie* driven by *Samcef*. *Oofelie* is a finite element multi-physics software which allows to model the couplings between various fields.

II. WORKING PRINCIPLE

The XBM magnetometer is based on a classical resonating xylophone bar. This relatively simple device uses the Lorentz force to measure one component of the ambient magnetic field. It consists of a thin conductive xylophone bar supported at the nodes of its fundamental mode of mechanical vibration by two arms bonded to the bar to provide low-resistance electrical contacts (see Figure 1). The nodes are located at 22.4% of the bar's length from each unclamped end. A sinusoidal current is supplied to the bar through these arms, oscillating at the fundamental transverse resonant mode of the bar. A first approximation of this frequency, considering a simple free-free bar, is given by

$$f_0 = \frac{22.4}{2\pi}\sqrt{\frac{EI_a}{\omega L^4}} = \frac{1.029b}{L^2}\sqrt{\frac{E}{\rho}} \qquad [1]$$

where E is the Young modulus (N/m^2), L the length of the bar, I_a the area moment of inertia ($= ab^3 / 12$ for a rectangular beam), ω the mass per unit length ($\rho = \omega\, a\, b$), and ρ, a, b are the mass density, width and thickness of the bar, respectively. When a current I is driven through the xylophone bar in the presence of an external magnetic field B_{ext}, a resulting Lorentz force applied to the bar makes it vibrate vertically, so that:

$$\vec{F} = I\vec{L}_s \wedge \vec{B}_{ext} \qquad [2]$$

where $\vec{L}$ is a vector whose magnitude Ls is the length of the xylophone bar between the supports ($Ls \sim 0.552\ L$). When the frequency of the current is set at the fundamental transverse resonant frequency of the bar, the deflection of the bar is strongly enhanced and a first approximation of its amplitude in the middle of the bar is given by

$$d(f_0) = \frac{5FL_s^4}{384EI_a}Q = 1.206\times10^{-3}\times\frac{FL^4}{EI_a}Q \qquad [3]$$

where Q is the mechanical quality factor which is determined by different parameters depending on bar material, manufacturing process, but also includes various types of dampings such as air damping, support damping, thermoelastic damping and surface damping. Equation [3] is obtained by modeling the bar as a mass-spring-dashpot system submitted to a static deformation.

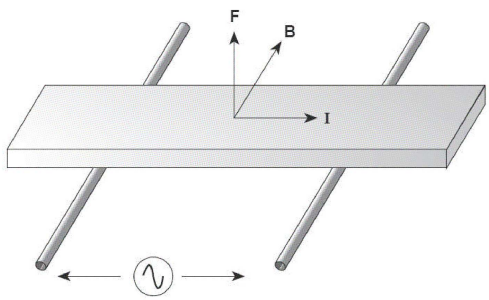

Fig. 1. Operating principle of a Xylophone Bar Magnetometer.

From equations [2], and [3], it can be seen that the amplitude of the deflection of the bar is linearly proportional to the magnetic field component *B* parallel to the surface of the xylophone bar and normal to the direction of the drive current. This device is therefore intrinsically linear unlike many other magnetometers. In principle, it also has a very wide dynamic range: magnetic field intensities from nanoteslas to teslas could be measured by simply adjusting the current amplitude. However, the maximum intensity of the current that can flow through the bar depends on the importance of the Joule effect and of the thermomechanical coupling. Indeed, a too large elevation of temperature inside the bar could result in significant modifications of its mechanical properties. Because the other vibration modes of the bar have a very different frequency and are not excited at this frequency f_0, this technique discriminates against these components of the magnetic field extremely well so that any second-order cross coupling between different field components is extremely small. A three-axis sensor can be constructed with three xylophone bars operating at different frequencies. The variation of the amplitude of the bar deflection as a function of the frequency of the driving current in a constant external magnetic field *B* is given by

$$d = d(f_0) \times \frac{1}{\sqrt{\left[1-\left(\frac{f}{f_0}\right)^2\right]^2 + \left(\frac{f}{Qf_0}\right)^2}} \qquad [4]$$

As the frequency is chosen as the fundamental mechanical resonance frequency, the displacement amplitude is enhanced, reaching a maximum value given by $d(f_0)$, while the phase angle displays a 180° shift.

III. PIEZOELECTRIC DETECTION

An efficient technique to measure the deflection of the vibrating bar is to use piezoelectric material. For the two designs presented in this section, the piezoelectric material is Lead Zirconate Titanate (PZT) which has been used extensively for years. There are several ways to include this material into the design. The most common one is to place the PZT layer between two platinum layers which act as electrodes, as in (Zakar et al 2003). Another way, which, to the knowledge of the authors, has not been reported so far, is to use only one Platinum layer and to place the PZT layer at the same level, as described in sub-section III. B.

A. Design 1

A design using Pt/PZT/Pt sandwich structure has been simulated and is presented in this sub-section. The length and width of the bar are 2500 µm and 250 µm, respectively and the dimensions of the four linkages are 5 µm x 50 µm. These arms are placed at the nodes of the fundamental mode of mechanical vibration of the bar. The base of the structure is made of 3 µm of silicon and 0.2 µm of silicon dioxide on top of it. On top of that structure, there is the Pt/PZT/Pt sandwich structure of thickness 0.25 µm, 1 µm and 0.25 µm, respectively.The whole structure (vibrating bar and linkages) is made of the same layers and has the same cross-section. A top view and a cross-sectional view of the magnetometer are depicted in Figures 2(a) and 2(b), respectively.

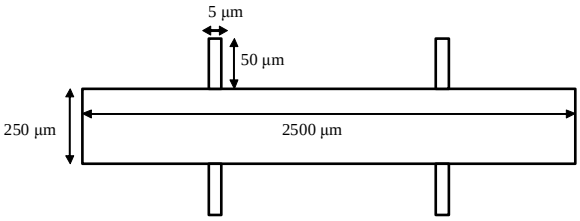

(a)

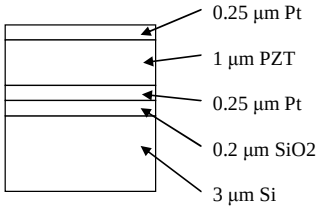

(b)

Fig. 2. Drawing depicting top view (a) and cross-sectional view (b) of the simulated model

A sinusoidal current oscillating at the fundamental transverse resonant mode of the bar is injected through the linkages. It is flowing along the bar through the doped silicon. The SiO2 layer acts as an insulator. According to Equation [2], the amplitude of the deflection is proportional to the intensity of the injected current. Therefore, in order to reach a high sensitivity, a strong current should flow through the bar. Nevertheless, as mentioned in Section II, the increase of temperature should not be excessive. For this reason, we limit the intensity of the current to a value which leads to an increase of temperature (due to Joule effect) of 100 K. For this structure, the maximum injected current is 5.6 mA and the voltage applied between the linkages is 4 V. The distribution of the current density in the bar obtained with Oofelie by solving an electrokinetic problem is shown in Fig. 3.

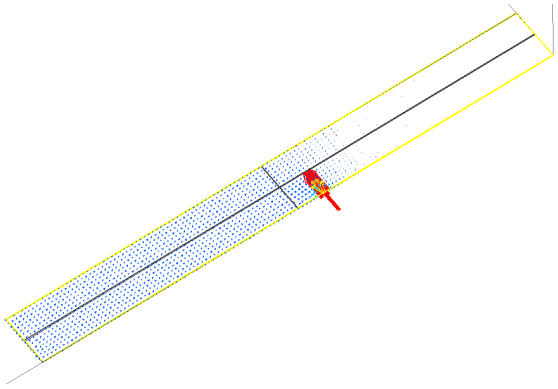

Fig. 3. Distribution of the current density in the bar. Only one quarter of the structure is shown.

At its first eigenfrequency (6956 Hz), for a current of 5.6 mA and in a magnetic field of 1 nT, the maximum deflection of the bar is 144 e-12 m and the difference of potential between the two electrodes is 1 µV. In this simulation, only thermo-elastic damping is taken into account. This approximation is realistic since this magnetometer is designed to be used in space. Figure 4 illustrates the deformation of the bar when vibrating at its fundamental transverse resonant mode.

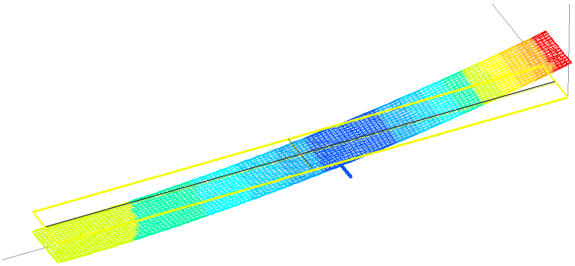

Fig. 4. Deformation of the bar when vibrating at its fundamental transverse resonant mode. Only one quarter of the structure is shown.

B. Design 2.

In order to increase significantly the amplitude of the voltage that is measured, a new structure has been designed. Since the difference of potential between two opposite faces of a PZT structure is proportional to the thickness or width of the structure (depending on how it is deposited), it is of interest to have a structure as thick (or wide) as possible. On the other hand, the thicker the bar, the smaller the amplitude of the deflection. Therefore, in the new design the electrodes are not placed below and above the PZT like in the first design, but are placed on each side of the PZT, at the two extremities of the bar. The bottom electrode has to be removed in order not to short-circuit the side electrodes and the PZT. Thus, the two electrodes at the extremity of the bar are made with the same Pt layer. A top view and a cross-sectional view of the new design are depicted in Figure 5(a) and 5(b), respectively. The dimensions of the bar as well as those of the linkages are similar to the dimensions of the first design. The base of the structure is still made of 3 µm of silicon and 0.2 µm of silicon dioxide on top of it. On top of that structure, there are only the PZT and Pt layers of thickness 0.25 µm each. The PZT is deposited only in the center of the bar. The width of the PZT does not affect the amplitude of the voltage. This configuration allows the electrical connection between the side electrodes and the linkages.

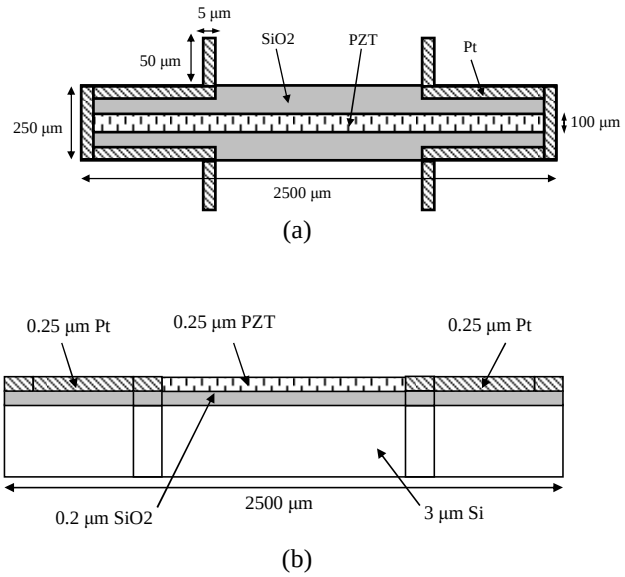

Fig. 5. Drawing depicting top view (a) and cross-sectional view (b) of the simulated model

For the same reason as for the first structure, the voltage applied between the linkages is set to 4V and the current flowing through the silicon is 5.6 mA. The distribution of the current density is similar to the one of the first design. At its first eigenfrequency and in a magnetic field of 1 nT, the maximum deflection of the bar is 320e-12 m and the difference of potential between the two electrodes is 6 mV. The electric potential distribution on the surface of the PZT is shown in Fig. 6. In this simulation also, only thermo-elastic damping is taken into account.

From these simulations it can be seen that the new design is about 6000 times more sensitive than the design which uses traditional Pt/PZT/Pt structure. This design has been simulated in magnetic fields from 0.1 nT up to 10e3 nT and it has been noticed that both the amplitude of the vibration and the output voltage

from the PZT are linear over the entire range. In a magnetic field of 0.2 nT, the output voltage from the PZT is 1.2 mV, which is the limit of what can be measured by the sensor electronics. Therefore, the expected sensitivity of the magnetometer is about 0.2 nT.

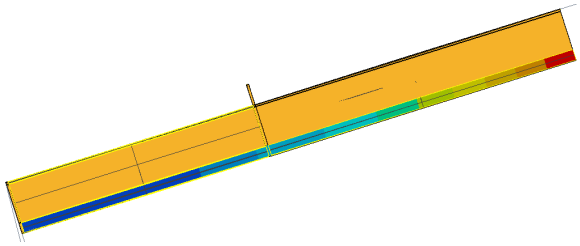

Fig. 6. Electric potential distribution on the surface of the PZT. Only one quarter of the structure is shown.

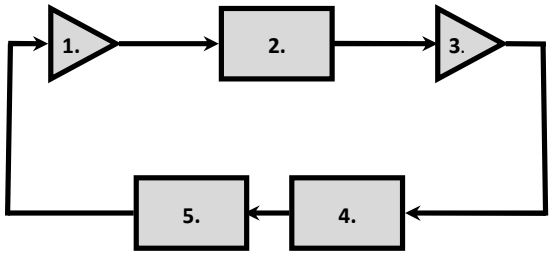

1. High output current Amplifier (Iout = 5.6 mA, Vout = 4V)
2. Device under test: MEMS magnetometer
3. Low noise amplifier (Vin = 3mV)
4. Analog to digital converter
5. Digital control Unit

Fig. 7. Bloc diagram of the proposed electronic circuit.

C. Sensor electronics

One of the prerequisite to achieve the sensitivity mentioned in the previous sub-section is that the supplied current must oscillate exactly at the eigenfrequency of the bar. This frequency will fluctuate due to several factors such as temperature and pressure. Therefore, it is necessary to have an electronic circuit with closed-loop feedback to control both the intensity and frequency of the supplied current. A bloc diagram of the proposed control/readout circuit is depicted in Fig. 7. In order to decrease the power consumption, a separate sigma delta analog-to-digital converter (ADC) (box 4 in Fig. 7) with small number of bits is used to sample the output voltage of the low noise amplifier (box 3). Therefore, in order to have a good accuracy with a minimum number of bits, the digital control unit (box 5) includes an automatic gain control (AGC) which ensures that the ADC will not be out of range. Another advantage of this AGC is that it will decrease the current injected into the bar when the magnetic field increase and therefore will decrease the power consumption of the high output current amplifier (box 1).

IV. CAPACITIVE DETECTION

The principle of the capacitive detection method is that by vibrating, the bar changes a capacitance which is part of an electronic resonating circuit such as ring resonator. Then, a change in the capacitance introduces a change in the resonance frequency. Therefore, the measurement of the magnetic field is achieved by measuring a frequency shift. To change the capacitance, two electrodes have to move relatively to each other. Since one electrode is the vibrating bar, the second electrode has to be either below, above or on the side. Because it is usually not possible to have a second electrode above or below with traditional MEMS technologies, we have designed a structure with electrodes on each side of the bar. In order to increase the change of capacitance when the bar is vibrating, an inter-digit structure has been designed. A 3-D view of the model when no current is supplied is plotted in Figure 8. In that Figure, the blue part is the vibrating bar and the red parts on each side are the static electrodes. Figure 9 illustrates the structure when vibrating at its fundamental transverse resonant mode. It can be seen that the capacitance decreases as the magnetic field increases. A first version of this design, using only a 3 µm silicon layer for the vibrating bar has been simulated but, due to the small amplitude of the deflection, the change in capacitance is too small and leads to an undetectable frequency shift. Therefore, another design, which includes a metallic layer on top of the vibrating bar has to be simulated.

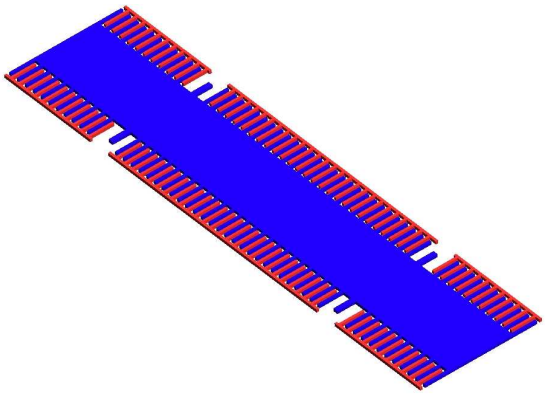

Fig. 8. 3-D view of the model. No current supplied.

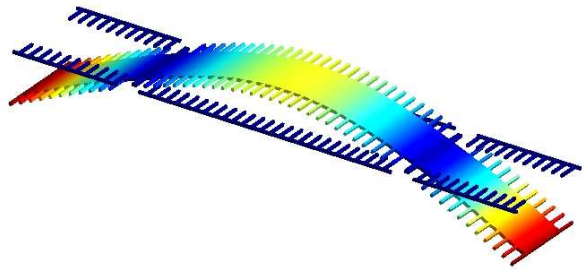

Fig. 9. Deformation of the bar when vibrating at its fundamental transverse resonant mode.

V. CONCLUSIONS AND PERSPECTIVES

In the Space Physics community, an increasing need to carry out multi-point measurements exists, in particular for magnetic field measurements. This is true for both scientific and space weather applications. The current trend is to develop and launch a set of micro-, nano- or pico-satellites carrying a small and light payload with small energy consumptions needs. With these requirements in mind, we initiated a study to design a MEMS xylophone bar magnetometer which fulfills these conditions.

In this study, it is clearly seen that the new configuration of the PZT/electrodes structure proposed in this paper leads to much higher sensitivity than traditional Pt/PZT/Pt structures. Sensitivity in the order of 0.2 nT is reported. The principle of the sensor electronics which ensures the optimal sensitivity and power consumption of the XBM is presented.

In addition, a design using capacitive detection with lateral inter-digit electrodes is introduced. When the vibrating bar is made of only one silicon layer, the amplitude of the vibration of the bar is too small to lead to a measureable frequency shift. Therefore, another version of the design, which includes a metallic layer on top of the silicon layer has to be tested.

The current which flows through the vibrating bar increases the temperature of the structure. The results reported in (Requier 2010) indicate that multiphysics couplings can have a negative impact on the mechanical quality factor and therefore can decrease the sensitivity of the device. Therefore, further simulations and measurements are needed to evaluate more precisely the impact of this coupling on the performance of the magnetometer.

ACKNOWLEDGMENT

The authors would like to thank Stéphane Paquay from *Open Engineering* for his numerous advices on how to carry out and improve the FEM simulations with Oofelie.

REFERENCES

[1] Givens R.B. et al, A high sensitivity, wide dynamic range magnetometer
designed on a xylophone resonator, Appl. Phys. Lett. 69 (18), 2755-2757, 1996.

[2] Wickenden D.K. et al, Development of miniature magnetometers, John Hopkins APL Technical Digest, Volume 18, Number 2, 1997.

[3] Zanetti L.J. et al, Miniature magnetic field sensors based on xylophone resonators, Science closure and Enabling technologies for Constellation Class Missions, edited by V. Angelopoulos and P.V. Panetta, 149-151, UC Berkeley, Californie, 1998.

[4] D.A. Oursler et al, Development of the Johns Hopkins Xylophone Bar Magnetometer, John Hopkins APL Technical Digest, Volume 20, Numero 2, 1999.

[5] Wickenden D.K. et al, Micromachined polysilicon resonating xylophone
bar magnetometer, Acta Astronautica 52, 421-425, 2003.

[6] Zakar E. et al, PZT MEMS for an Extremely Sensitive Magnetometer, Integrated Ferroelectrics, 54, 697-706, 2003.

[7] Requier S., Harmonic Simulation of a MEMS Xylophone Bar Magnetometer : multiphysics couplings and validation of electrokinetic thermoelastic elements in Oofelie™, Master thesis in order to obtain a Master of Engineering degree in Astronautics and Aeronautics at the University of Liège, 2010.